IEEE Access
Multidisciplinary | Rapid Review | Open Access Journal

Received July 15, 2019, accepted August 7, 2019, date of publication August 14, 2019, date of current version August 28, 2019.

Digital Object Identifier 10.1109/ACCESS.2019.2935208

A Matched Negative Group Delay Circuit and Its Integration With an Unequal Power Divider

JIAN-KANG XIAO[1], QIU-FEN WANG[1], AND JIAN-GUO MA[2], (Fellow, IEEE)
[1]School of Electro-Mechanical Engineering, Xidian University, Xi'an 710071, China
[2]School of Computers, Guangdong University of Technology, Guangzhou 510006, China

Corresponding author: Jian-Guo Ma (mjg@gdut.edu.cn)

This work was supported in part by the National Natural Science Foundation of China under Grant 61871458, in part by the National Natural Science Foundation of Shaanxi Province under Grant 2018JM6027, and in part by the Guangdong Innovative and Entrepreneurial Research Team Program and the AoShan Talents Program Supported by the Qingdao National Laboratory for Marine Science and Technology.

ABSTRACT In this paper, a resonator coupling negative group delay (NGD) circuit with resistor-loaded coupled lines is presented firstly, and then an unequal Wilkinson power divider with NGD characteristic is designed by integrating the proposed NGD circuit into an unequal power divider. Both the NGD circuit and the unequal power divider with NGD characteristic have been fabricated and measured, and both of the designs have been demonstrated. The proposed NGD circuit has a measured signal attenuation (S_{21}) of 13.5 dB, a S_{11} attenuation of 31.7 dB, and a negative group delay time of −2.56 ns, while the proposed integration circuit has a measured S_{11}/S_{33} attenuation of more than 37 dB, a S_{22} attenuation of more than 22 dB, an isolation of more than 35 dB, and a negative group delay time of −4.21 ns.

INDEX TERMS Negative group delay circuit, resistor-loaded coupled lines, unequal power divider, integration.

I. INTRODUCTION

With the rapid development of communication technology, group delays (GDs) of microwave radars and telecommunication systems have been paid more and more attention because of the long delays and signal distortion. In order to overcome such problems, GD compensation is commonly required for improving group delay flatness or phase linearity. NGD circuit is an effective way to compensate for the positive group delay and decrease the variation of the passband group delay. The NGD characteristic, which causes the output peak to precede the input peak, had been applied in some microwave circuits design, such as shortening or reducing delay lines in feed-forward amplifiers to improve efficiency and bandwidth [1], minimizing beam-squint delay flatness in phased array antennas [2], eliminating phase variation with frequency in broadband constant phase shifters [3], realizing non-Foster reactive elements [4], and producing negative group delay characteristic in power dividers (PDs) [5], and couplers [6], [7], et al. Both passive and active NGD circuits had been developed.

Commonly, NGD circuits are designed by using the signal attenuation characteristics of a bandstop filter [8]–[12], however, large losses and reflection wave would be accompanied if unmatched. In recent years, absorptive [10] and self-matched techniques [12] had been developed to enhance the attenuation of S_{11} for reducing the reflection wave to the source, which is helpful to overcome the undesired standing wave and instability problem of the microwave system terminal. It is known that there are two types of bandstop filters, one is stub/resonator-loaded type, and the other is resonator-feed line coupling type. Both types can be used for NGD circuits design. In this research, we note that the resonator-feed line coupling structure is more flexible to realize the desired NGD circuit because the coupling gap between the resonator and feed line is helpful to enhance the attenuation of S_{11}, so this type of structure is selected in this paper.

Power dividers [13]–[16] are important components for power dividing and combining, which have wide applications in radar systems and wireless communications such as high power amplifiers, mixers, and antenna feeding networks. PDs are also essential components in some measurement instrumentation such as network analyzer. The conventional PDs have positive group delay [17], which would bring negative influences on the performance of microwave/millimeter-wave circuits and systems. PD with

The associate editor coordinating the review of this article and approving it for publication was Kuang Zhang.

NGD characteristic [18]–[20] would compensate a positive group delay and eliminate the delay compensation element and attenuator, which is very useful for the pre-distortion amplifier to enhance the circuit linearity.

In this paper, a simple NGD circuit with resistors connected coupled lines without requiring external matching networks has been designed firstly, and then it is integrated with an unequal power divider as replacing transmission path 3-1 by the NGD circuit to generate negative group delay characteristic. Both the proposed NGD circuit and the integration circuit have been fabricated, and the designs have been demonstrated by experiment. The NGD circuit has a measured signal attenuation (S_{21}) of 13.5 dB, a S_{11} attenuation of 31.7 dB, and a negative group delay bandwidth of 110 MHz ($\tau = 0$), while the unequal power divider with NGD characteristic has a measured $S_{11}/S_{22}/S_{33}$ attenuation of no less than 22.7 dB, signal attenuation of no more than 16.85 dB, and an isolation of more than 35 dB.

This paper is organized as follows. Firstly, a NGD circuit with resistor-loaded coupled lines is designed, analyzed by transmission line theory, and implemented. Secondly, an unequal power divider with negative group delay characteristic is schemed by integrating the NGD circuit with a power divider, and the NGD part of the integration circuit is analyzed by coupling topology. Thirdly, the integration circuit is realized, and the performance is compared and discussed. Both the NGD circuit and the integration circuit have been fabricated and demonstrated by experiment. Finally, a conclusion is drawn.

II. A MATCHED NEGATIVE GROUP DELAY CIRCUIT DESIGN

A matched negative group delay circuit is proposed by a feeding line coupling with a pair of resonators which generates NGD characteristic, and a pair of port matched networks which absorb the reflection waves, as is shown in Figure 1. The schemed circuit structure is constructed by a 50Ω feeding line, a pair of uniform impedance resonators (UIRs), and a pair of resistor (R_1) loaded parallel coupled lines which are used to realize port matching. The coupling gap between the resonator and feed line would be helpful for adjusting the attenuation of S_{11}.

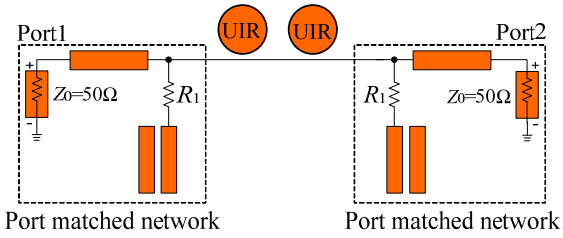

FIGURE 1. A matched coupling type negative group delay circuit scheme.

The transmission line model of the NGD circuit can be achieved according to the design scheme, as is shown in Figure 2(a). Where Z_1 is the feeding line with characteristic impedance of 50Ω, Z_2 is the characteristic impedance of the UIRs, Z_{o3} and Z_{e3} are the corresponding odd/even-mode characteristic impedances of the parallel coupled lines. θ_i ($i = 1, 2, 3$) is the electric length corresponding to the i-th transmission line, and $\theta_i = (l_i\omega\sqrt{\varepsilon_{re}})/c$. Here l_i is the physical length of the i-th microstrip line, ω is the angular frequency, ε_{re} is the effective permittivity, and c is the velocity of light in free space. C_1 denotes the coupling capacitance between the resonator and the feeding line. By laying a magnetic wall and an electric wall on TT', respectively, the even-mode and the odd-mode equivalent circuits can be obtained, as are plotted in Figure 2(b) and (c), respectively.

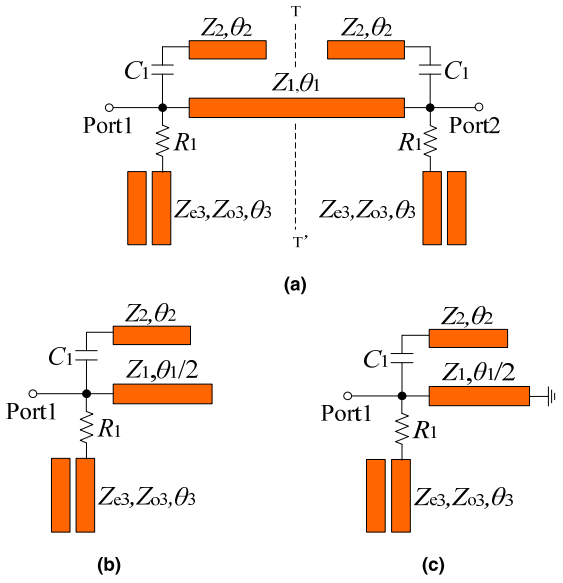

FIGURE 2. Transmission line model of the proposed matched NGD circuit and its even/odd-mode circuits. (a) Transmission line model of the NGD circuit. (b) even-mode circuit. (c) Odd-mode circuit.

For the resonator coupling with feeding line structure, gap capacitance C_1 can be seen as a series capacitance of the resonator with characteristic impedance of Z_2, as is shown in Figure 3. C_1 can be obtained when the resonance occurs as

$$C_1 = -\frac{1}{Z_2\omega_0 \cot\theta_2} \tag{1}$$

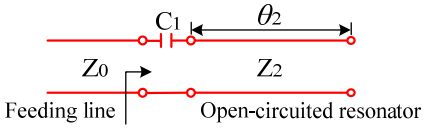

FIGURE 3. Equivalent circuit of the gap coupling resonator.

A. EVEN/ODD- MODE ANALYSIS

For the even-mode circuit as shown in Figure 2(b), the circuit input admittance can be expressed as

$$Y_{ine} = Y_1^e + Y_2^e + Y_3^e \tag{2}$$

where Y_1^e, Y_2^e and Y_3^e are the admittances of each branch, and can be respectively formulated according to the transmission line and circuit theory as

$$Y_1^e = \frac{j\omega C_1}{1 + Z_2\omega C_1 \cot\theta_2} \tag{3}$$

$$Y_2^e = -\frac{1}{jZ_1 \cot(\frac{\theta_1}{2})} \tag{4}$$

$$Y_3^e = \frac{y_{11}y_{22} - y_{12}y_{21}}{R_1(y_{11}y_{22} - y_{12}y_{21}) + y_{22}} \tag{5}$$

In (5), y_{11}, y_{12}, y_{21} and y_{22} are the admittance matrix elements of the open-circuited coupled lines, and the admittance matrix can be expressed as

$$[Y] = \begin{bmatrix} y_{11} & y_{12} \\ y_{21} & y_{22} \end{bmatrix} = \frac{1}{|Z|}\begin{bmatrix} -j\frac{1}{2}(Z_{e3} + Z_{o3})\cot\theta_3 & j\frac{1}{2}(Z_{e3} - Z_{o3})\csc\theta_3 \\ j\frac{1}{2}(Z_{e3} - Z_{o3})\csc\theta_3 & -j\frac{1}{2}(Z_{e3} + Z_{o3})\cot\theta_3 \end{bmatrix} \tag{6}$$

$|Z|$ in (6) is the determinant of the impedance matrix [Z] of the open-circuited coupled lines. [Z] can be formulated as

$$[Z] = \begin{bmatrix} -j\frac{1}{2}(Z_{e3} + Z_{o3})\cot\theta_3 & -j\frac{1}{2}(Z_{e3} - Z_{o3})\csc\theta_3 \\ -j\frac{1}{2}(Z_{e3} - Z_{o3})\csc\theta_3 & -j\frac{1}{2}(Z_{e3} + Z_{o3})\cot\theta_3 \end{bmatrix} \tag{7a}$$

$$Z_{e3} = Z_3\sqrt{(1 + C)/(1 - C)} \tag{7b}$$

$$Z_{o3} = Z_3\sqrt{(1 - C)/(1 + C)} \tag{7c}$$

here C is the coupling coefficient of the coupled lines. If we define $M = 4R_1$, $N = (Z_{e3} + Z_{o3})\cot\theta_3$, $P = 1 + Z_2\omega C_1 \cot\theta_2$, the input admittance of the even-mode circuit can be expressed as

$$Y_{\text{ine}} = \frac{M}{N^2 + M} + j[\frac{2N}{N^2 + M} + \frac{\omega C_1}{P} + \frac{\tan(\frac{\theta_1}{2})}{Z_1}] = a + jb \tag{8}$$

For the odd-mode circuit as illustrated in Figure 2(c), the circuit input admittance can be expressed as

$$Y_{ino} = Y_1^o + Y_2^o + Y_3^o \tag{9}$$

The admittance of each odd-mode circuit branch can be expressed respectively as

$$Y_1^o = \frac{j\omega C_1}{1 + Z_2\omega C_1 \cot\theta_2} \tag{10}$$

$$Y_2^o = \frac{1}{jZ_1 \tan(\frac{\theta_1}{2})} \tag{11}$$

$$Y_3^o = \frac{y_{11}y_{22} - y_{12}y_{21}}{R_1(y_{11}y_{22} - y_{12}y_{21}) + y_{22}} \tag{12}$$

The input admittance of the odd-mode circuit can be obtained as

$$Y_{\text{ino}} = \frac{M}{N^2 + M} + j[\frac{2N}{N^2 + M} + \frac{\omega C_1}{P} - \frac{\cot(\frac{\theta_1}{2})}{Z_1}] = a + jc \tag{13}$$

According to the even/odd-mode analysis and network theory, the circuit S parameters can be expressed as [21]

$$S_{11} = S_{22} = \frac{Y_0^2 - Y_{ine}Y_{ino}}{(Y_0 + Y_{ine})(Y_0 + Y_{ino})} \tag{14}$$

$$S_{12} = S_{21} = \frac{Y_0(Y_{ino} - Y_{ine})}{(Y_0 + Y_{ine})(Y_0 + Y_{ino})} \tag{15}$$

where $Y_0 = 1/Z_0$, $Z_0 = 50\Omega$. For port matching with $S_{11} = S_{22} = 0$, we get

$$Y_0^2 - a^2 - bc + ja(b + c) = 0 \tag{16}$$

with

$$a = \frac{M}{N^2 + M} \tag{17a}$$

$$b = \frac{2N}{N^2 + M} + \frac{\omega C_1}{P} + \frac{\tan(\frac{\theta_1}{2})}{Z_1} \tag{17b}$$

$$c = \frac{2N}{N^2 + M} + \frac{\omega C_1}{P} - \frac{\cot(\frac{\theta_1}{2})}{Z_1} \tag{17c}$$

From the matching condition as expressed in (16), it is seen that the matching is not only depending on the resistor-loaded coupled lines, but also related with the coupling resonator, C_1 and Z_1.

The circuit transmission coefficient can be obtained by (8), (13) and (15) as

$$S_{12} = S_{21} = \frac{jY_0(c - b)}{(Y_0 + a)^2 - bc + j(Y_0 + a)(b + c)} \tag{18}$$

The circuit group delay time can be obtained by

$$\tau = -\frac{d\angle S_{21}}{d\omega} \tag{19}$$

Of course, when the port matching network is not considered, the input admittance of the even-mode and the odd-mode can be simplified as $Y_{\text{ine}} = Y_1^e + Y_2^e$, $Y_{\text{ino}} = Y_1^o + Y_2^o$, respectively, and the corresponding S parameters can be obtained by formulas (14) and (15).

B. CIRCUIT IMPLEMENTATION

The NGD circuit is specified as centering at 5.2 GHz with NGD time of −1.6 ns, NGD bandwidth of 150 MHz ($\tau = 0$), return loss (RL) of 33 dB, and insertion loss (IL) of 12 dB. The circuit can be implemented by the design scheme as shown in Figure 1, the transmission line model and the theoretical analysis of (1)-(19). The electric parameters of the UIR can be obtained by the circuit specifications and the resonance condition as $Z_2 = 115.6\Omega$, $\theta_2 = 4.02$ rad, and $C_1 = -0.251$ pF. Here the gap capacitance C_1 gets negative value because of the non-Foster effect [4]. The design flowchart has been illustrated as that in Figure 4.

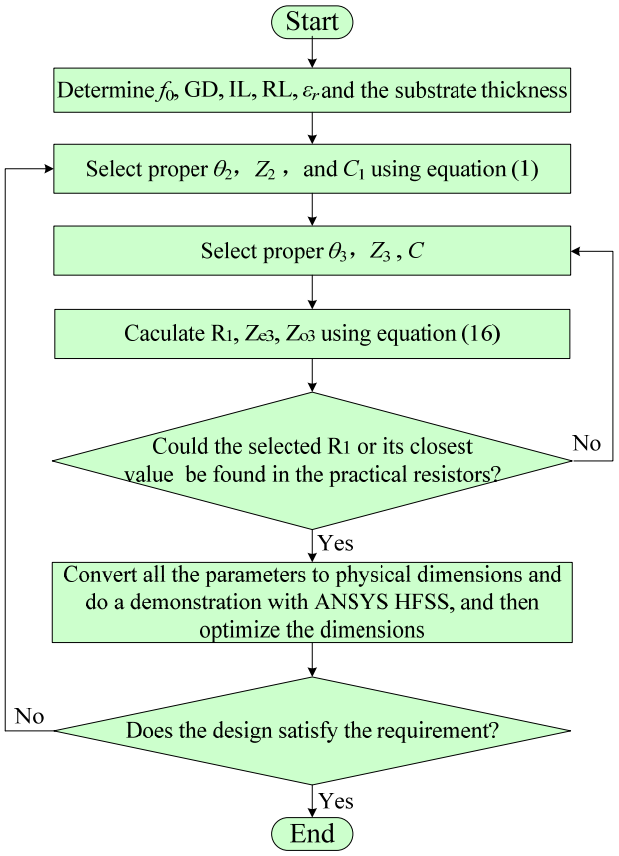

FIGURE 4. Design flowchart of the proposed negative group delay circuit.

When designing on a substrate with dielectric constant of $\varepsilon_r = 2.2$, and a thickness of 0.787 mm, the proposed NGD circuit structure can be obtained as that shown in Figure 5. The circuit size can be obtained by the design procedure as $w_1 = 2.46$, $w_2 = 0.5$, $w_3 = 0.5$, $w_4 = 1.1$, $s_0 = 0.2$, $l_1 = 18.2$, $l_2 = 8.4$, $l_3 = 1.4$, $l_4 = 5.0$, unit: mm. $R_1 = 80.6\ \Omega$.

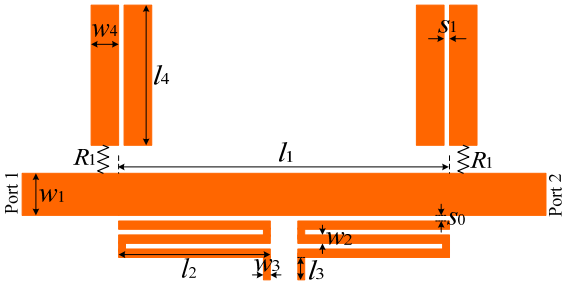

FIGURE 5. Physical structure of the proposed NGD circuit with resistor-loaded coupled lines.

For the certain dimensions, the simulated circuit frequency responses and group delay with and without port matching are plotted in Figure 6, where the frequency responses comparison is plotted in Figure 6(a), and the group delay comparison is shown in Figure 6(b). It can be seen clearly that with resistor-loaded coupled lines for port matching,

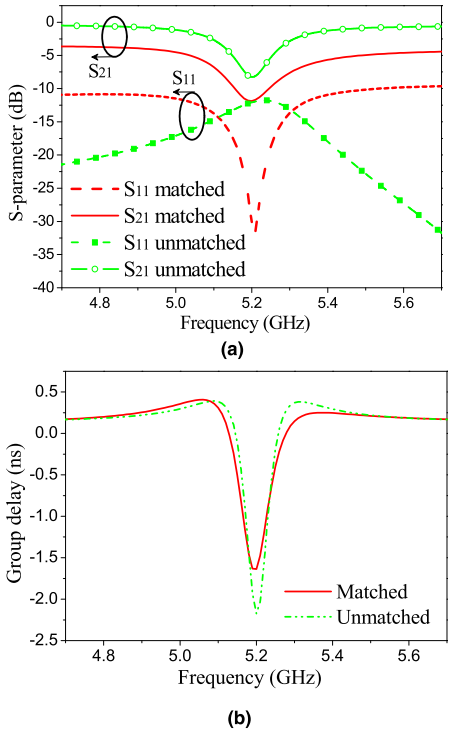

FIGURE 6. Simulated results comparison with and without port matching. (a) S_{11}/S_{21} comparison. (b) Group delay comparison.

reflection wave has been greatly attenuated from about 12 dB to 32 dB, while the center frequency keeps unchanged, and the insertion loss as well as negative group delay time only have slight variation. When centering at 5.2 GHz with the electric parameters of $Z_1 = 50\ \Omega$, $Z_2 = 115.6\ \Omega$, $Z_3 = 72.71\ \Omega$, $C_1 = -0.251$ pF, $\theta_1 = 2.73$ rad, $\theta_2 = 4.02$ rad, $\theta_3 = 0.733$ rad, and C = 0.318, insertion loss of the NGD circuit can be calculated as $S_{21} = -10.16$ dB, which is approaching to the simulated results of -12 dB, as is shown in Figure 6(a).

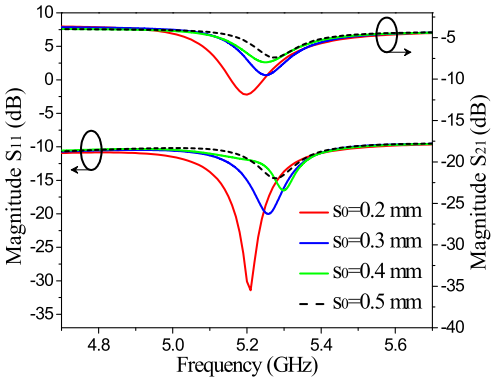

FIGURE 7. Frequency responses variation versus parameter s_0.

The simulated circuit frequency responses variations versus parameters s_0, l_3 and external resistor R_1 are plotted in Figures 7, 8, and 9, respectively. It is seen from

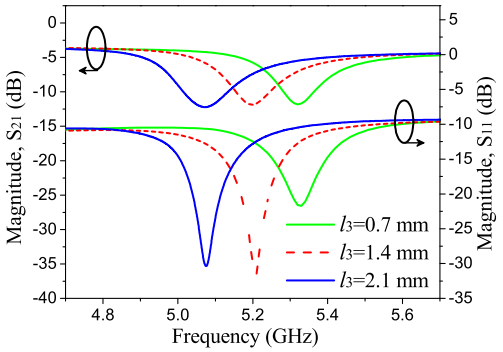

FIGURE 8. Frequency responses variation versus l_3.

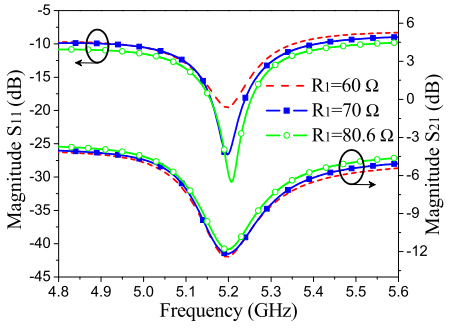

FIGURE 9. Frequency responses variation versus resistor R_1.

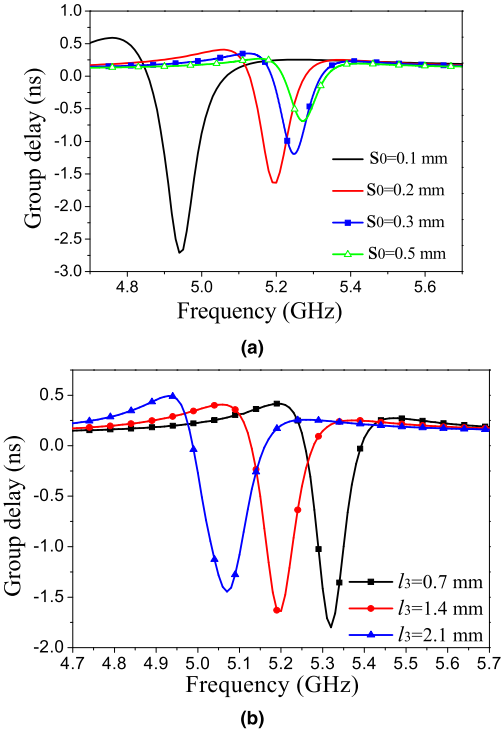

FIGURE 10. Group delay variation versus parameters s_0 and l_3. (a) GD variation versus s_0. (b) GD variation versus l_3.

Figure 7 that S_{11}/S_{21} can be controlled simultaneously by the coupling gap s_0, and both of the magnitude of S_{11} and S_{21} increases with s_0 decreasing. It is noted that the attenuation of S_{11} enhances greatly to be more than 30 dB when the coupling gap decreases to be 0.2 mm. Figure 8 shows that l_3 nearly has no effect on S_{21}, but controls the circuit center frequency importantly, which decreases obviously with l_3 increasing. Figure 9 indicates that resistor R_1 has little effect on S_{21}, but the attenuation of S_{11} increases obviously with R_1 increasing. Simulated group delay variations versus parameters s_0 and l_3 are illustrated in Figure 10(a) and (b), respectively. It can be seen that smaller coupling gap introduces bigger group delay time, while the UIR size such as l_3 only has unsignificant effect on group delay time. When the coupling gap changes from 0.2 mm to 0.1 mm, the negative group delay time increases obviously from -1.63 ns to -2.71 ns.

In this research, it is also noted that the resistor-loaded coupled lines have little effect on group delay, but more effect on the circuit center frequency, except for an important role on S_{11} attenuation. The attenuation of S_{11} increases with the coupled lines length decreasing.

It is concluded from the above analysis that 1) circuit center frequency is dominantly controlled by the UIR dimension, on the other hand, s_0 and l_4 also have some effect on the circuit center frequency. 2) S_{11} can be controlled/adjusted by the coupling gap s_0, and the resistor loaded coupled lines, of course including resistor R_1. 3) The group delay time and signal attenuation (S_{21}) can be adjusted by s_0. In order to obtain a larger group delay time, a smaller s_0 is preferred, however, which would bring more signal attenuation, and higher fabrication precision is also required.

C. EXPERIMENTAL RESULTS

The proposed matched NGD circuit is fabricated, as is shown in Figure 11(a), and the experimental results are shown in Figure 11(b) and (c), respectively. It is seen that the proposed NGD circuit has a measured center frequency of 5.28 GHz with a signal attenuation (S_{21}) of 13.5 dB, a reflection coefficient attenuation of 31.7 dB, a group delay time of -2.56 ns, and a negative group delay bandwidth of 110 MHz ($\tau = 0$), which approaches to the simulated results but has a working frequency shift, which is due to the material permittivity tolerance and the fabrication uncertainty. Since the variation of S_{21} is relevance with the variation of group delay, as that is formulated in (19), so compared with the simulated results, it is seen that an increased measured S_{21} accompanies with more NGD time. The proposed NGD circuit has a circuit size of 28.2 mm $\times$ 12.5 mm($0.67\lambda_g \times 0.30\lambda_g$), where λ_g is the guided wavelength at 5.2 GHz.

III. A UNEQUAL POWER DIVIDER WITH NEGATIVE GROUP DELAY CHARACTERISTIC

A. CIRCUIT DESIGN

Commonly, a power divider has positive group delay. In this research, an unequal power divider with negative group delay characteristic is proposed based on the presented negative group delay circuit integration with unequal Wilkinson power divider. The design scheme is that the NGD characteristic can

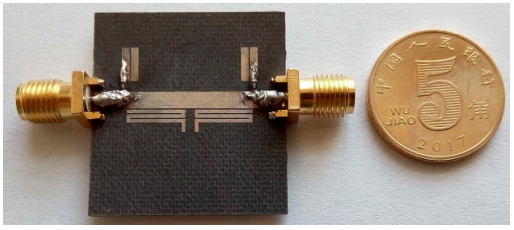

(a)

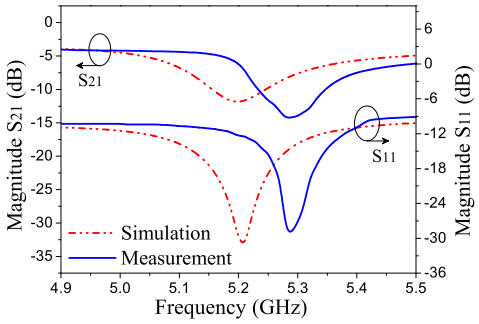

(b)

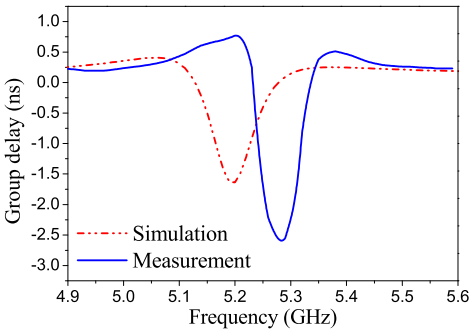

(c)

FIGURE 11. Fabrication and measured results. (a) Fabricated hardware. (b) Measured and simulated S_{11}/S_{21} comparison. (c) Measured and simulated group delay comparison.

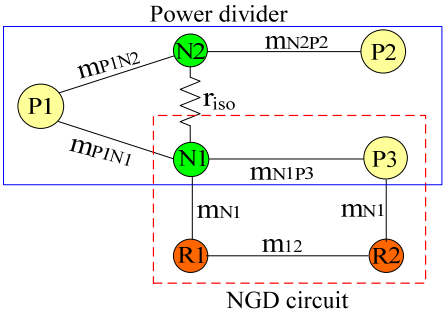

FIGURE 12. Coupling topology of the schemed power divider with NGD characteristic [18].

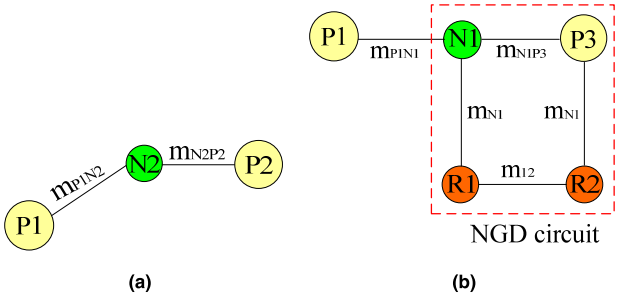

(a) (b)

FIGURE 13. Coupling topology of the even-mode. (a) Coupling structure of port1 to port2. (b) Coupling structure of port1 to port3.

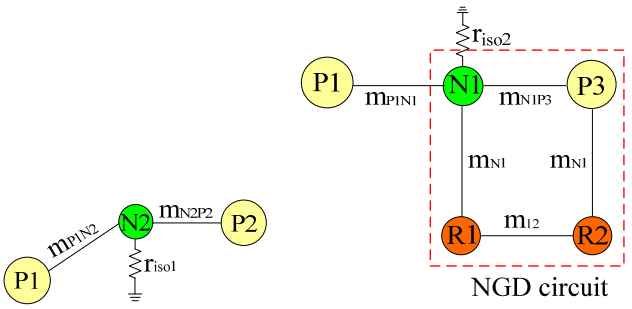

(a) (b)

FIGURE 14. Coupling topology of the odd-mode. (a) Coupling structure of port1 to port2. (b) Coupling structure of port1 to port3.

be generated by transmission route 1-3 (port1-port3), while the resistor-loaded coupled lines are used to attenuate S_{11} for obtaining a good matching. The coupling topology of the integration circuit is shown in Figure 12, where P1, P2 and P3 represent port 1, port 2 and port 3, respectively. N1 and N2 denote the non-resonant nodes, $r_{\rm iso}$ is the normalized isolation resistor, while R1 and R2 denote the UIRs. m represents the coupling coefficient of each part.

The even-mode and the odd-mode coupling topologies can be achieved when the even-mode and the odd-mode are excited, respectively, as are illustrated in Figure 13 and 14, respectively. Where the Coupling structures from port1 to port2 are shown in Figure 13(a) and Figure 14(a), while that from port1 to port3 are shown in Figure 13(b) and Figure 14(b). $r_{\rm iso1}$ and $r_{\rm iso2}$ are the equivalent normalized isolation resistors for transmission routes 1-2 and 1-3, respectively, when the odd-mode is excited. Let $r_{\rm iso1} = k^2$, $r_{\rm iso2} = 1$, the total normalized isolation resistor can be expressed as $r_{\rm iso} = 1 + k^2$, and the practical isolation resistor can be obtained as

$$R_{iso} = \frac{1 + \mathrm{k}^2}{k} Z_0 \tag{20}$$

The unequal power divider with NGD characteristic is designed centering at 5.2 GHz with a fractional bandwidth of 1.5%, a negative group delay time of $\tau_{31} = -5$ ns, power division ratio of $k = 0.9$, and a unloaded quality factor $Q_{\rm u} = 115$. For these specifications and $a = 0.3$, the normalized coupling matrix of the NGD circuit [18] section

TABLE 1. Comparison of this work and the related reports.

Ref.	k^2	S_{11} (dB)	S_{22} (dB)	S_{33} (dB)	S_{21} (dB)	S_{31} (dB)	S_{23} (dB)	τ_{21} (ns)	τ_{31} (ns)	NGD-BW (MHz)/f_0 (GHz)
[5]	1	-30.38	-26.76	-28.99	-9.29	-9.30	-42.18	-1.16	-1.17	-/2.14
[18]	0.6	-21.97	-18.98	-17.93	-2.26	-9.96	-39.12	0.32	-0.866	60/2.14
[18]	1	-19.92	-18.26	-17.79	-3.21	-8.701	-33.97	0.31	-0.828	60/2.14
[18]	2	-20.86	-17.46	-19.73	-4.98	-7.48	-33.4	0.34	-0.851	60/2.14
[19]	1	-28.9	-17.5	-18.2	-6.95	-6.97	-15.8	-0.54	-0.56	-/2.138
[20]	1	-24.73	-20.58	-20.62	-2.96	-24.35	-42.18	0.34	-0.529	-/2.14
ours	0.81	-37.6	-22.7	-37.67	-4.23	-16.85	-35.06	0.14	-4.21	73/5.26

composed by N1, R1, R2 and P3 can be formulated as

$$M_{NGD} = \begin{bmatrix} 0 & 0.6 & 0 & 0.91 \\ 0.6 & -j/1.725 & 0.108 & 0 \\ 0 & 0.108 & -j/1.725 & 0.6 \\ 0.91 & 0 & 0.6 & 0 \end{bmatrix} \quad (21)$$

where $m_{N1} = 0.6$, $m_{12} = 0.108$, $m_{NIP3} = 0.91$. The more detailed calculation of the coupling matrix is shown in the Appendix. The other coupling coefficients can be calculated as $m_{P1N1} = 0.669$, $m_{P1N2} = 0.826$, and $m_{N2P2} = 1.111$.

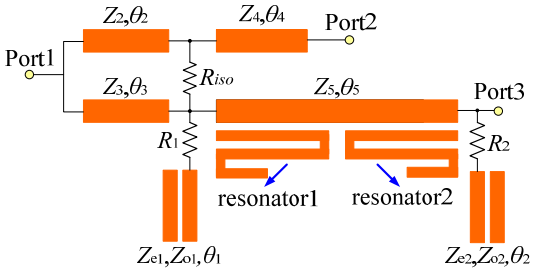

FIGURE 15. Transmission line circuit model of the unequal power divider with NGD characteristic.

According to the design scheme and the coupling topology of the power divider with negative group delay characteristic, the transmission line circuit model can be constructed as that shown in Figure 15. The circuit characteristic impedances can be expressed according to the unequal Wilkinson power divider as

$$Z_2 = Z_0\sqrt{k(1+k^2)} \quad (22a)$$

$$Z_3 = Z_0\sqrt{\frac{(1+k^2)}{k^3}} \quad (22b)$$

$$Z_4 = Z_0\sqrt{k} \quad (22c)$$

$$Z_5 = \frac{Z_0}{\sqrt{k}} \quad (22d)$$

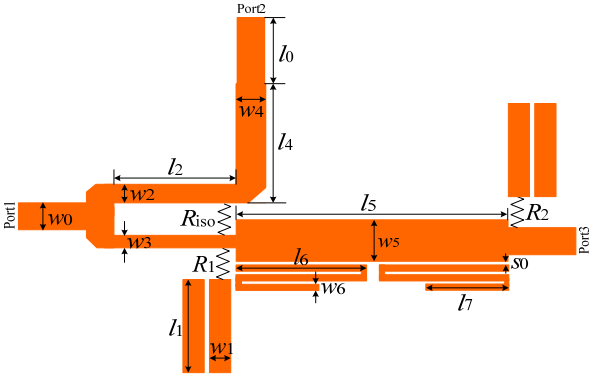

FIGURE 16. Physical structure of the proposed unequal power divider with NGD characteristic.

For the certain power division ratio, the corresponding characteristic impedance of each section can be obtained by formulas (22a)-(22d) as $Z_2 = 63.82\ \Omega$, $Z_3 = 78.78\ \Omega$, $Z_4 = 47.43\ \Omega$, and $Z_5 = 52.70\ \Omega$, here $Z_0 = 50\ \Omega$. The physical structure of the proposed unequal power divider with NGD characteristic can be realized by the transmission line model and the theoretical analysis, as that shown in Figure 16. The circuit dimensions can be obtained by the circuit specifications, the coupling matrix, the characteristic impedances of the unequal Wilkinson power divider with certain power division ratio, and the theoretical analysis of the NGD circuit as $w_0 = 2.4$ mm, $l_0 = 5$ mm, $w_1 = 1.2$ mm, $l_1 = 5.4$ mm, $w_2 = 1.65$ mm, $l_2 = 10.6$ mm, $w_3 = 1.1$ mm, $l_3 = 10.6$ mm, $w_4 = 2.6$ mm, $l_4 = 10.6$ mm, $w_5 = 2.6$ mm, $l_5 = 20.5$ mm, and $l_6 = 9.8$ mm. $R_{iso} = 101.7\ \Omega$, $R_1 = R_2 = 100\ \Omega$. The circuit is implemented on a substrate with dielectric constant of 2.2, and a thickness of 31 mils.

B. PERFORMANCE COMPARISON AND ANALYSIS

For the certain dimension of the proposed power divider with NGD characteristic, the simulated S parameters and group delay variations versus coupling gap s_0 is shown in Figure 17.

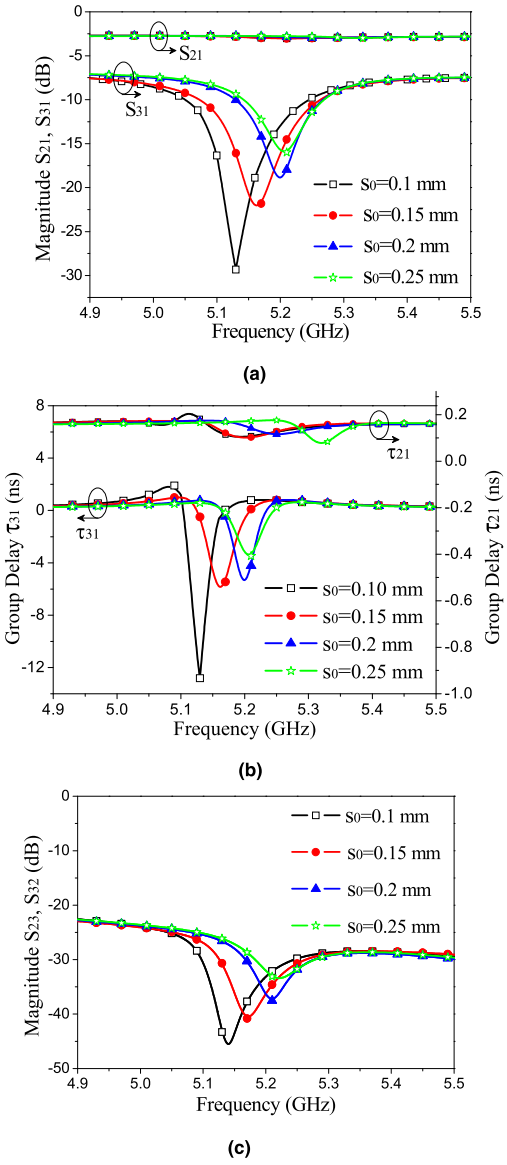

FIGURE 17. Simulated frequency responses of the unequal power divider with NGD characteristic versus parameter s_0. (a) S_{21}/S_{31} versus s_0. (b) Group delay versus s_0. (c) Isolation S_{23}/S_{32} versus s_0.

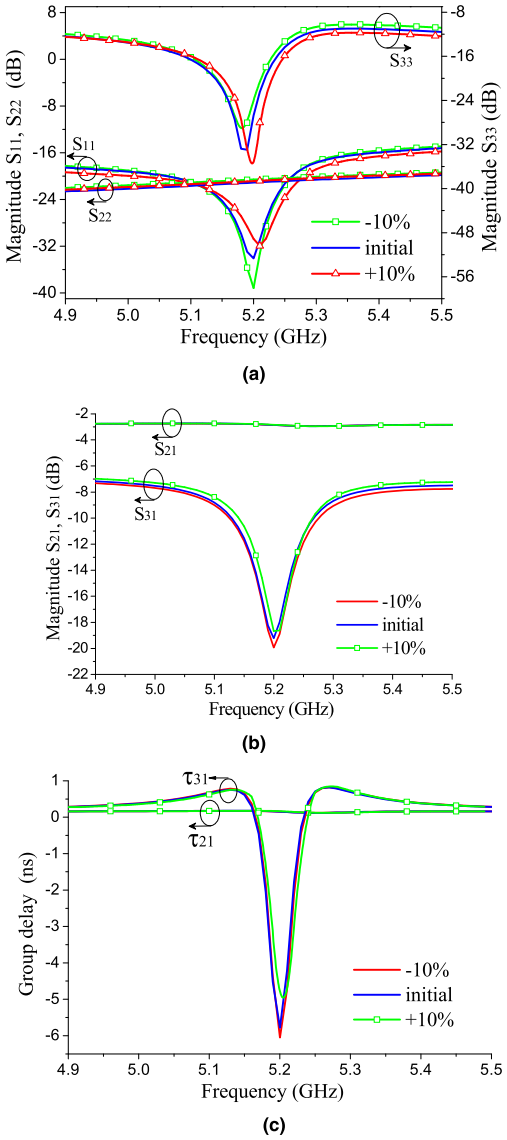

FIGURE 18. S parameters and group delay variation of the unequal power divider versus resistor R_1/R_2. (a) $S_{11}/S_{22}/S_{33}$ versus R_1/R_2. (b) S_{21}/S_{31} versus R_1/R_2. (c) Group delay versus R_1/R_2. Initial $R_1 = R_2 = 100\Omega$.

It can be seen from Figure 17(a) and (b) that when s_0 increases from 0.1 mm to 0.25 mm, S_{21} and τ_{21} only have nonsignificant change, but S_{31} and τ_{31} decrease with s_0 increasing. The variation of τ_{31} is relevance with the variation of S_{31}. It is for that when s_0 increases, the coupling between UIR and the node N1 as well as P3 becomes weaker, which makes m_{N1} decrease. It also can be seen that a larger s_0 brings an increased center frequency. It is noted from Figure 17(c) that PD isolation decreases with s_0 increasing, which is because that the PD isolation is related with the power division ratio k and the reflection coefficient from port 2 and port 3, while the reflection coefficient decreases with s_0 increasing, as that has been demonstrated in Figure 7. As S_{31} decreases with s_0 increasing, while S_{21} nearly fixing, and for $k = S_{31}/S_{21}$, it can be concluded that the power division ratio may be changed with the variation of s_0, and the practical power division ratio would decrease with s_0 increasing.

Simulated S parameters and group delay versus resistors R_1/R_2 are plotted in Figure 18(a)-(c). For the initial resistance value of $R_1 = R_2 = 100\ \Omega$, it can be seen that the magnitude of S_{11}/S_{33} vary about ± 7 dB corresponding to the variation of R_1/R_2 within $\pm 10\%$, while S_{22} has no obvious change, as that is shown in Figure 18(a). It is seen from Figure 18(b) and (c) that the variation of R_1/R_2 bring a S_{31} variation of ± 1.3 dB, and a τ_{31} variation of ± 1 ns, while S_{21} and τ_{21} nearly keeping fixed. It can be concluded that S_{31} and τ_{31} are not sensitive to the variation of R_1/R_2.

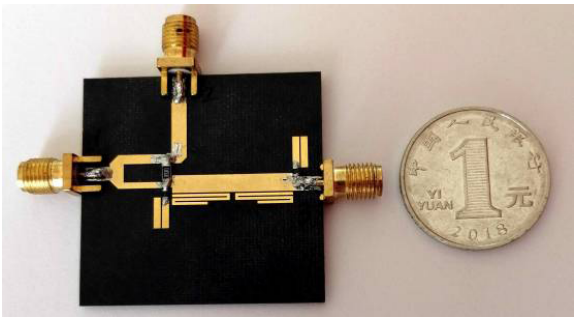

FIGURE 19. Fabricated hardware of the unequal power divider with NGD characteristic.

C. EXPERIMENT AND DISCUSSION

The proposed unequal power divider with NGD characteristic has been fabricated, as is shown in Figure 19. The experimental results by Agilent E5071C vector network analyzer are shown in Figure 20, where the comparison of the simulated and measured S_{21}/S_{31} are shown in Figure 20(a), the comparison of the simulated and measured group delay are shown in Figure 20(b), the comparison of the simulated and the measured $S_{11}/S_{22}/S_{33}$ are plotted in Figure 20(c), while the measured and the simulated isolation are illustrated in Figure 20(d). Measurement approaches to the simulation. It can be seen from the measurement that the integration circuit centers at 5.26 GHz with $S_{31} = -16.85$ dB, $S_{21} > -4.23$ dB, $\tau_{31} = -4.21$ ns, and $\tau_{21} < 0.14$ ns, which approach to the simulated results of $S_{31} = -18.8$ dB, $S_{21} = -2.86$ dB, $\tau_{31} = -5.3$ ns, and $\tau_{21} = 0.13$ ns. The measured power division ratio is more than 12.6 dB. It can be seen from Figure 20(c) that the measured $S_{33}/S_{22}/S_{11}$ at the center frequency are no less than -37.67 dB, -22.7 dB, and -37.6 dB, respectively, which are similar with the simulated results of $S_{33} = -33$ dB, $S_{22} = -19.8$ dB, and $S_{11} = -33.8$ dB, respectively. Figure 20(d) indicates that the measured isolation is $S_{23} = S_{32} = -35.06$ dB, which is approaching to the simulated result of -37.5 dB. The discrepancy between measurement and simulation is mainly the frequency shift, which is due to the material permittivity tolerance, fabrication uncertainty, and the resistance error. The integration circuit of the unequal power divider with negative group delay characteristic has a size of $0.86\lambda_g \times 0.52\lambda_g$(36.2 mm × 21.9 mm), where λ_g is the guided wavelength at 5.2 GHz.

Comparison of this work and the related reports is listed in Table 1, where k^2 denotes the power division ratio of the power divider without the NGD circuit, and NGD-BW is the negative group delay bandwidth. It can be seen that the proposed unequal power divider with NGD characteristic has more reflection wave attenuation than [5], [18], [19] and [20], less insertion loss of S_{21} than [5] and [19], less insertion loss of S_{31} than [20], higher isolation than [18] and [19], less group delay time of τ_{21} than [18] and [20], more negative group delay than [5], [18]–[20], and wider negative group delay bandwidth as well as higher center frequency than [5], [18]–[20].

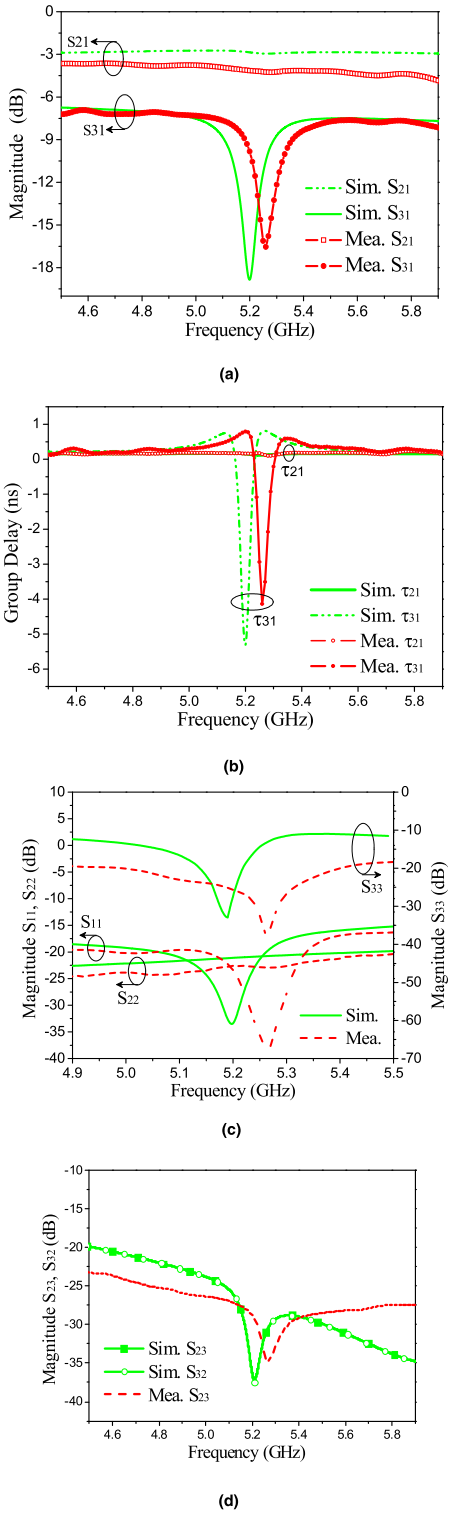

FIGURE 20. Measured results of the unequal PD with NGD characteristic. (a) Simulated and measured S_{21}/S_{31} comparison. (b) Simulated and measured group delay comparison. (c) Simulated and measured $S_{11}/S_{22}/S_{33}$ comparison. (d) Simulated and measured isolation comparison. Sim.-Simulated, Mea.-Measured.

IV. CONCLUSION

In this paper, a negative group delay circuit based on resistor-loaded coupled lines and resonator coupling scheme

$$m_{12} = a m_{N1}^2 \tag{24}$$

$$m_{NIP3} = \frac{a m_{N1}^4 \mp \sqrt{a^2 m_{N1}^8 + (a^2 m_{N1}^4 + \frac{1}{Q_u^2\Delta^2})\left[m_{N1}^4(a^2-1) + \frac{1}{Q_u^2\Delta^2}\right]}}{a^2 m_{N1}^4 Q_u^2 \Delta^2 + 1} \times Q_u^2\Delta^2 \tag{25}$$

is presented, and the NGD circuit has been used to integrate with an unequal Wilkinson power divider to generate NGD characteristic. The NGD characteristic of the integrated circuit can be well controlled by the resistor-loaded coupled lines which introduce port matching. For the integration circuit, group delay which associates with the NGD circuit (transmission path 3-1) is negative, while the group delay which associates with transmission path 2-1 is positive. Of course, the NGD characteristic also can be obtained if transmission path 2-1 integrates to the NGD circuit. Both of the proposed NGD circuit and the unequal power divider with NGD characteristic have been fabricated and measured, and the experimental results approach to the predictions. The presented NGD circuit and the integration circuit have advantages of simple circuit structures, good reflection coefficient attenuation, high isolation, and negative group delay effect, which would be promising for applications of minimizing the influence of the positive group delay in the RF circuit design.

APPENDIX

For the transmission path from P1 to P3 as is shown in Figure 12, the coupling matrix can be expressed as [18]

$$\boldsymbol{M}_{\mathrm{NGD}} = \begin{array}{c} \\ \mathrm{N1} \\ \mathrm{R1} \\ \mathrm{R2} \\ \mathrm{P3} \end{array} \begin{array}{c} \begin{array}{cccc} \mathrm{N1} & \mathrm{R1} & \mathrm{R2} & \mathrm{P3} \end{array} \\ \begin{bmatrix} 0 & m_{N1} & 0 & m_{N1P3} \\ m_{N1} & -\dfrac{j}{Q_u\Delta} & m_{12} & 0 \\ 0 & m_{12} & -\dfrac{j}{Q_u\Delta} & m_{N1} \\ m_{N1P3} & 0 & m_{N1} & 0 \end{bmatrix} \end{array} \tag{23}$$

where m_{N1} is an assumed value [18], Q_{u} is the unloaded quality factor which can be extracted by simulator, Δ is the 3 dB fractional bandwidth, and a is a positive constant. m_{12} and m_{N1P3} can be formulated as that in (24) and (25), as shown at the top of this page, respectively. In (25), the positive sign is selected when $m_{\mathrm{N1}} > 0$, whereas the negative sign is selected when $m_{\mathrm{N1}} < 0$. In this design, m_{N1} is defined as a positive value.

REFERENCES

[1] H. Noto, K. Yamauchi, M. Nakayama, and Y. Isota, "Negative group delay circuit for feed-forward amplifier," in *Proc. IEEE/MTT-S Int. Microw. Symp.*, Honolulu, HI, USA, Jun. 2007, pp. 1103–1106.

[2] S. S. Oh and L. Shafai, "Compensated circuit with characteristics of lossless double negative materials and its application to array antennas," *IET Microw., Antennas Propag.*, vol. 1, no. 1, pp. 29–38, Feb. 2007.

[3] B. Ravelo, M. Le Roy, and A. Pérennec, "Application of negative group delay active circuits to the design of broadband and constant phase shifters," *Microw. Opt. Technol. Lett.*, vol. 50, no. 12, pp. 3078–3080, Dec. 2008.

[4] H. Mirzaei and G. V. Eleftheriades, "Realizing non-Foster reactive elements using negative group delay networks," *IEEE Trans. Microw. Theory Techn.*, vol. 61, no. 12, pp. 4322–4332, Dec. 2013.

[5] G. Chaudhary and Y. Jeong, "A design of power divider with negative group delay characteristics," *IEEE Microw. Wireless Compon. Lett.*, vol. 25, no. 6, pp. 394–396, Jun. 2015.

[6] Y. Wu, H. Wang, Z. Zhuang, Y. Liu, Q. Xue, and A. A. Kishk, "A novel arbitrary terminated unequal coupler with bandwidth-enhanced positive and negative group delay characteristics," *IEEE Trans. Microw. Theory Techn.*, vol. 66, no. 5, pp. 2170–2184, May 2018.

[7] B. Ravelo, "Theory of coupled line coupler-based negative group delay microwave circuit," *IEEE Trans. Microw. Theory Techn.*, vol. 64, no. 11, pp. 3604–3611, Nov. 2016.

[8] G. Chaudhary, Y. Jeong, and J. Lim, "Miniaturized dual-band negative group delay circuit using dual-plane defected structures," *IEEE Microw. Wireless Compon. Lett.*, vol. 24, no. 8, pp. 521–523, Aug. 2014.

[9] G. Chaudhary and Y. Jeong, "Transmission-type negative group delay networks using coupled line doublet structure," *IET Microw., Antennas Propag.*, vol. 9, no. 8, pp. 748–754, Jun. 2015.

[10] L.-F. Qiu, L.-S. Wu, W.-Y. Yin, and J.-F. Mao, "Absorptive bandstop filter with prescribed negative group delay and bandwidth," *IEEE Microw. Wireless Compon. Lett.*, vol. 27, no. 7, pp. 639–641, Jul. 2017.

[11] G. Liu and J. Xu, "Compact transmission-type negative group delay circuit with low attenuation," *Electron. Lett.*, vol. 53, no. 7, pp. 476–478, Mar. 2017.

[12] T. Shao, Z. Wang, S. Fang, H. Liu, and S. Fu, "A compact transmission-line self-matched negative group delay microwave circuit," *IEEE Access*, vol. 5, pp. 22836–22843, 2017.

[13] X. Ren and K. D. Xu, "Multilayer balanced-to-unbalanced power divider with wideband transmission characteristic and common-mode suppression," *IEEE Trans. Compon., Packag., Manuf. Technol.*, vol. 9, no. 1, pp. 72–79, Jan. 2019.

[14] B. Li, X. Wu, and W. Wu, "A vol. 10, p. 1unequal wilkinson power divider using coupled lines with two shorts," *IEEE Microw. Wireless Compon. Lett.*, vol. 19, no. 12, pp. 789–791, Dec. 2009.

[15] Y. Wu, Y. Liu, and Q. Xue, "An analytical approach for a novel coupled-line dual-band wilkinson power divider," *IEEE Trans. Microw. Theory Techn.*, vol. 59, no. 2, pp. 286–294, Feb. 2011.

[16] C. Miao, J. Yang, G. Tian, X. Zhang, and W. Wu, "Novel sub-miniaturized Wilkinson power divider based on small phase delay," *IEEE Microw. Wireless Compon. Lett.*, vol. 24, no. 10, pp. 662–664, Oct. 2014.

[17] M.-C. J. Chik and K.-K. M. Cheng, "Group delay investigation of rat-race coupler design with tunable power dividing ratio," *IEEE Microw. Wireless Compon. Lett.*, vol. 24, no. 5, pp. 324–326, May 2014.

[18] G. Chaudhary and Y. Jeong, "Negative group delay phenomenon analysis in power divider: Coupling matrix approach," *IEEE Trans. Compon., Packag., Manuf. Technol.*, vol. 7, no. 9, pp. 1543–1551, Sep. 2017.

[19] G. Chaudhary, P. Kim, J. Jeong, and Y. Jeong, "A design of negative group delay power divider: Coupling matrix approach with finite unloaded-Qu resonators," in *Proc. IEEE MTT-S Int. Microw. Symp. (IMS)*, San Francisco, CA, USA, May 2016, pp. 1–3.

[20] G. Chaudhary, J. Park, Q. Wang, and Y. Jeong, "A design of unequal power divider with positive and negative group delays," in *Proc. Eur. Microw. Conf. (EuMC)*, Paris, France, Sep. 2015, pp. 127–130.

[21] J. Hong and M. J. Lancaster, *Microstrip Filters for RF/Microwave Applications*. Hoboken, NJ, USA: Wiley, 2001.

JIAN-KANG XIAO received the B.S. degree in electronics and the M.S. degree in radio physics from Lanzhou University, China, in 1996 and 2004, respectively, and the Ph.D. degree from Shanghai University, China, in 2007. He was a Postdoctoral Research Fellow with the South China University of Technology, China, from 2007 to 2009. He was with Hohai University, China, from 2009 to 2011. He then joined Xidian University, China. He was an Academic Visitor with Tianjin University, China, and Heriot-Watt University, U.K., from 2013 to 2014 and 2015 to 2016, respectively. His research interests include microwave passive components design and antennas. He was a Reviewer of many international journals, including the IEEE TRANSACTIONS ON MTT, IEEE MWCL, *IEEE Microwave Magazine*, IEEE ACCESS, IET MAP, and *Electronics Letters* (IET).

QIU-FEN WANG was born in Henan, China. She received the B.S. degree in measurement and control technology and instrumentation from the North China University of Water Resources and Electric Power, China, in 2016. She is currently pursuing the M.S. degree with Xidian University, China. Her research interest includes microwave negative group delay circuit design.

JIAN-GUO MA received the B.Sc. and M.Sc. degrees from Lanzhou University, China, in 1982 and 1988, respectively, and the Ph.D. degree in engineering from Duisburg University, Germany, in 1996.

He was a Postdoctoral Fellow with the Technical University of Nova Scotia (TUNS), Halifax, NS, Canada, from 1996 to 1997. He was a Faculty Member with Nanyang Technological University (NTU), Singapore, from October 1997 to November 2005, where he was also the Founding Director of the Center for Integrated Circuits and Systems. From 2005 to 2009, he was with the University of Electronic Science and Technology of China (UESTC), China. He then joined Tianjin University, China. He is currently a Professor with the Guangdong University of Technology. His research interests include RFICs and RF integrated systems for wireless, RF device characterization modeling, MMIC, and RF/microwave circuits and systems design. He was a recipient of the prestigious Changjiang (Yangtze) Chair Professorship awarded by the Ministry of Education of China, in 2008. He was also the Distinguished Young Investigator awarded by the National Natural Science Foundation of China, in 2008.